INFECTION AND IMMUNITY, Feb. 2007, p. 565–573 Vol. 75, No. 2
0019-9567/07/$08.00+0 doi:10.1128/IAI.01479-06

Enteropathogenic *Escherichia coli*, *Shigella flexneri*, and *Listeria monocytogenes* Recruit a Junctional Protein, Zonula Occludens-1, to Actin Tails and Pedestals▽†

Miyuki Hanajima-Ozawa,[1] Takeshi Matsuzawa,[2] Aya Fukui,[1] Shigeki Kamitani,[1] Hiroe Ohnishi,[1] Akio Abe,[2] Yasuhiko Horiguchi,[1] and Masami Miyake[1]*

Department of Molecular Bacteriology, Research Institute for Microbial Diseases, Osaka University, 3-1 Yamadaoka, Suita-city, Osaka 565-0871, Japan,[1] and Laboratory of Bacterial Infection, Kitasato Institute for Life Sciences, Kitasato University, 5-9-1 Shirokane, Minato-ku, Tokyo 108-8642, Japan[2]

Received 15 September 2006/Returned for modification 4 November 2006/Accepted 14 November 2006

Enteropathogenic *Escherichia coli*, *Shigella flexneri*, and *Listeria monocytogenes* induce localized actin polymerization at the cytoplasmic face of the plasma membrane or within the host cytoplasm, creating unique actin-rich structures termed pedestals or actin tails. The process is known to be mediated by the actin-related protein 2 and 3 (Arp2/3) complex, which in these cases acts downstream of neural Wiskott-Aldrich syndrome protein (N-WASP) or of a listerial functional homolog of WASP family proteins. Here, we show that zonula occludens-1 (ZO-1), a protein in the tight junctions of polarized epithelial cells, is recruited to actin tails and pedestals. Immunocytochemical analysis revealed that ZO-1 was stained most in the distal part of the actin-rich structures, and the incorporation was mediated by the proline-rich region of the ZO-1 molecule. The direct clustering of membrane-targeted Nck, which is known to activate the N-WASP–Arp2/3 pathway, triggered the formation of the ZO-1-associated actin tails. The results suggest that the activation of the Arp2/3 complex downstream of N-WASP or a WASP-related molecule is a key to the formation of the particular actin-rich structures that bind with ZO-1. We propose that an analysis of the recruitment on a molecular basis will lead to an understanding of how ZO-1 recognizes a distinctive actin-rich structure under pathophysiological conditions.

A dramatic reorganization of cytoskeletal proteins in mammalian cells is a common response to infections by certain pathogenic bacteria (20). Some of the bacteria produce unique actin-rich structures within distinct regions on the cytoplasmic face of the plasma membrane or within the cytoplasm of the infected host cells (20, 49). Enteropathogenic *Escherichia coli* (EPEC), *Shigella flexneri*, and *Listeria monocytogenes* exemplify the bacteria organizing such unique actin-rich structures. EPEC induces the formation of membranous protrusions, termed "pedestals," on the surface of the intestinal epithelial cells (24, 38). On the other hand, *S. flexneri* and *L. monocytogenes* (40, 41) induce the formation of the elongated actin-rich structures termed actin tails within the host cytosol (5, 53). The EPEC-induced formation of pedestals is triggered by two bacterial factors, intimin and Tir (translocated intimin receptor) (28). Tir is one of the virulence factors termed "effectors," which are delivered directly into the host cytoplasm through bacterial secretion machinery termed the type III secretion system (TTSS) (24, 46). The secreted Tir is in turn integrated into the plasma membrane and binds with a bacterial outer membrane protein, intimin (31). The binding induces the clustering of the membrane-associated Tir beneath the bacteria, which activates an Nck adaptor molecule at the cytoplasmic face of the plasma membrane and finally results in activation of neural Wiskott-Aldrich syndrome protein (N-WASP) and the downstream actin-nucleating Arp2/3 complex (19, 23). Actin polymerization induced by *S. flexneri* is mediated by a bacterial outer membrane protein, IcsA/VirG (5). The protein directly binds and activates N-WASP, which leads to the Arp2/3 complex-dependent actin tail formation (30, 51). In contrast, a listerial outer membrane protein, ActA, does not bind with Nck or N-WASP, but instead directly binds with Arp2/3, through the ActA region shared with WASP family proteins. This region mimics the activity of WASP, thereby creating actin tails attached to one pole of a bacterial cell (6, 30, 49, 58). Thus, a signal through N-WASP or a WASP-related molecule is considered to be a common feature for the formation of actin-rich structures, although the bacterial elements triggering the formation differ in different bacteria. The actin-rich structures contain a variety of actin-binding and cytoskeletal proteins, as well as the F-actin filaments as a major structural component (for review, see reference 49). Some of the proteins are essential (8, 9, 29, 51, 58), while others are nonessential but affect the efficiency (3, 12, 35, 45, 47, 52) of the formation and function of the structures. Thus, these proteins should participate in the coordinated regulation of actin dynamics to create the actin-rich structures, although a full understanding of their precise roles still requires further investigation.

In the course of analyzing the pathogenesis of EPEC, we found that the bacteria recruit zonula occludens-1 (ZO-1) to

* Corresponding author. Mailing address: Department of Molecular Bacteriology, Research Institute for Microbial Diseases, Osaka University, 3-1 Yamadaoka, Suita-city, Osaka 565-0871, Japan. Phone: 81-6-6879-8285. Fax: 81-6-6879-8283. E-mail: mami@biken.osaka-u.ac.jp.

† Supplemental material for this article may be found at http://iai.asm.org/.

▽ Published ahead of print on 21 November 2006.

the actin-rich structures that they have created. It is well known that ZO-1 generally concentrates at intercellular tight junctions and is not accumulated in other actin-rich structures such as stress fibers and filopodia. This implies that ZO-1 may play a role in the production, maintenance, or other functions of the bacterium-created actin-rich structures. In this study, we describe the mechanism by which ZO-1 is recruited in the pedestal produced by EPEC and that a similar recruitment is observed with *S. flexneri* and *L. monocytogenes*. Results presented here indicate that three pathogenic bacteria, EPEC, *Shigella*, and *Listeria*, recruited ZO-1 to the actin-rich structures through a similar mechanism. We propose that certain pathogenic bacteria create particular actin-rich structures that attract ZO-1 through a signal generated by WASP-related molecules.

MATERIALS AND METHODS

Plasmid. The oligonucleotide primers used for the amplification of DNA fragments are listed in Table 1. The C terminus of mouse ZO-1 (CZO-1, encompassing amino acids 507 to 1746) and truncated mutants, which were tagged with a monomeric enhanced green fluorescence protein (mEGFP) at their N termini, were constructed as follows. First, the gene for mEGFP was amplified by PCR using template pBSII IRESmEGFP (a gift from Teruhito Yasui, Osaka University) and primer set mEGFP-F and mEGFP-R. The amplified fragment was cloned into the HindIII-EcoRV site of pcDNA3 (Invitrogen). The resulting plasmid was designated pcDNA3mEGFP-C. The DNA fragment encoding CZO-1, amplified by PCR using a template cDNA of mouse ZO-1 (a gift from Sho-ichiro Tsukita, Kyoto University) and the primers CZO-F and CZO-R, was cloned into the KpnI-EcoRI site of pcDNA3mEGFP-C. The resulting plasmid was designated pEGFP/CZO-1. Plasmids for the expression of truncated forms of CZO-1 except CZO-1ΔGuk were constructed by amplification of the respective DNA fragments by PCR using pEGFP/CZO-1 as a template and cloning the fragments into the KpnI-EcoRI site of pcDNA3mEGFP-C. The PCR primers used for each construct are as follows: for CZO-1ΔSH3, ΔSH3-F and ΔSH3-R; for CZO-1ΔPRR, ΔPRR-F and ΔPRR-R; and for CZO-1PRR, PRR-F and PRR-R. The plasmid pEGFP/CZO-1ΔGuk used for the expression of CZO-1ΔGuk was constructed by amplifying the DNA fragment (encoding amino acids 507 to 591 of ZO-1) by PCR with primers ΔGuk-F and ΔGuk-R and cloning it into the KpnI-HindIII site of pEGFP/CZO-1. The DNA fragment encoding the N terminus of ZO-1 (NZO-1; encompassing amino acids 1 to 506) tagged with a vesicular stomatitis virus glycoprotein (VSVG) epitope at its C terminus was amplified using a template cDNA of mouse ZO-1 with the primers NZO-F and NZO-R and cloned into the KpnI-EcoRI site of pcDNA3. DNA constructs encoding fused forms of CD16/7 with Nck SH3 domains and control plasmids were kindly provided by Bruce J. Mayer, University of Connecticut Health Center. The plasmid p99-tir for the expression of a wild-type Tir in *tir* -deficient mutant was described in a previous study (36). p99-tirY474F, a plasmid for the expression of a mutant Tir (Y474F), was generated from p99-tir using a Quick Change site-directed mutagenesis kit (Strategene) with the primers TirY474/F and TirY474/R.

Cell culture and transfection. HeLa and NIH 3T3 cells were maintained in Dulbecco's modified Eagle's medium (DMEM; Sigma) supplemented with 10% fetal bovine serum (FBS; Sigma). Caco/B7 cells were maintained in DMEM with 20% FBS. Caco/B7 is a subclone isolated from the Caco-2 human adenocarcinoma cell line by repeated cloning. We selected Caco/B7 from among 12 isolated subclones because it showed a relatively homogeneous morphology indistinguishable from that of the parental cells. The morphology appeared stable during 10 to 15 subcultures. Caco/B7 cells showed a higher transepithelial electrical resistance (TER) between apical and basolateral compartments when cultured on a collagen-coated permeable filter support (Transwell COL; Corning, Inc.) than other subclones. All of the cells were cultured in a CO_2 incubator at 37°C with an atmosphere of 5% CO_2–95% air.

For transfection experiments, HeLa and NIH 3T3 cells were plated on a coverslip (13 mm in diameter) in a 24-well plate at a density of 5×10^4 cells/well. After 18 to 20 h, plasmid DNA (400 ng) was transfected to the cells using Lipofectamine-Plus reagent (Invitrogen) by the method recommended by the manufacturer. The cells were incubated in DMEM–15% FBS for 21 h and infected with EPEC or treated with anti-CD16 antibody, as described below.

TABLE 1. Primers used in this study

Primer	Sequence[a]
mEGFP-F	5′-CCCAAGCTTGCCACCATGGTGAGCAAGGGCGAGG
mEGFP-R	5′-TGGATATCTTAGAATTCCTCGGTACCCTTGTACAGCTCGTCCATGCCGAGAGTG
CZO-F	5′-CGGGGTACCCCGTATCGCCGCATTGTAGAATCAG
CZO-R	5′-CGGAATTCTTAAAAGTGGTCAATCAGGACA
ΔSH3-F	5′-CGGGGTACCCCGTATCGCCGCATTGTAGAATCAG
ΔSH3-R	5′-CGGAATTCTTAAAAGTGGTCAATCAGGACA
ΔPRR-F	5′-CGGGGTACCCCGAAGACAGCGGGTGGTGATCGGG
ΔPRR-R	5′-CGGAATTCCGTTAAAGCTTATGAGAGCGTTCATATAGC
PRR-F	5′-GGGGTACCCGTAAGAACAATCACCATCTCTTCAC
PRR-R	5′-CGGAATTCTTAAAAGTGGTCAATCAGGACA
ΔGuk-F	5′-AATTAACCCTCACTAAAGGGAAC
ΔGuk-R	5′-GCCCAAGCTTTGGAAGTGTGTACTGTACACTGG
NZO-F	5′-CGGGGTACCCCGGCCACCATGTCCGCCAGGGCCGCGGCCGC
NZO-R	5′-CCGGAATTCCGGTTACTTGCCCAGCCTGTTCATCTCGATGTCGGTGTAAACATCCTTCTTCTTCTGAGCC
TirY474F/F	5′-GATCTGCGGCGACCTCATCAAAAATATGCTCTTCTGGC
TirY474/R	5′-GCCAGAAGAGCATATTTTTGATGAGGTCGCCGCAGATC

[a] Underlined sequences represent nucleotides specifying the restriction enzyme sites used for cloning.

Bacterial strains and infection experiments. E2348/69 (O127:K63:H6) is a wild-type strain of EPEC originally isolated from an epidemic case in England (27). Mutant strains were prepared from E2348/69 and have been reported elsewhere (33). *Shigella flexneri* 2a strain 15H405 and *Listeria monocytogenes* RIMD1205001 were obtained from the Osaka Prefectural Institute of Public Health and the International Research Center for Infectious Diseases, Pathogenic Microbes Repository Unit, Osaka University, respectively.

EPEC and the mutants were precultured at 37°C overnight in LB broth. *S. flexneri* cells were precultured at 37°C overnight in tryptose phosphate broth (Difco). Aliquots (120 μl) of the precultures were inoculated into 3 ml of DMEM and incubated for 3 h at 37°C in a CO_2 incubator. The bacterial suspensions were diluted with DMEM and subjected to infection experiments. *L. monocytogenes* precultured in brain heart infusion broth (Difco) at 37°C overnight were washed with 10 mM phosphate-buffered saline (PBS), pH 7.0, and promptly resuspended in DMEM for infection experiments as described below.

For the infection by EPEC, Caco/B7 cells were seeded on a polyester membrane support (Transwell Clear; Corning) in a 24-well plate at a density of 4.5×10^4 cells/well (0.33 cm^2) and incubated for 5 days. HeLa cells (0.8×10^5 to 1.0×10^5 cells/well) were plated on a coverglass (13-mm diameter) in a 24-well plate at 37°C overnight. The cells were infected with EPEC at a multiplicity of infection (MOI) of 15 to 20 for 1 h in a CO_2 incubator. Nonadherent bacteria were washed with prewarmed DMEM, and the cells were incubated at 37°C thereafter. When HeLa cells were infected, the incubation was paused at 2 h, and additional incubation for 3 h was performed to promote pedestal elongation in the presence of gentamicin at a final concentration of 100 μg/ml.

For the infection by *S. flexneri* or *L. monocytogenes*, HeLa cells (0.8×10^5 to 1.0×10^5 cells/well) on a coverglass dipped in a 24-well plate with serum-free DMEM were infected with bacteria at MOIs of 100 for *S. flexneri* and 50 to 80 for *L. monocytogenes*. The culture plates were centrifuged at $700 \times g$ for 10 min at room temperature to enhance bacterial contact with the host cells. After 30 min at 37°C, the plates were washed three times and then incubated in DMEM–

10% FBS containing 100 μg/ml gentamicin for 2 to 3 h (*S. flexneri*) or 3 to 4 h (*L. monocytogenes*) at 37°C in a CO_2 incubator.

Induction of artificial Tir-intimin interaction by intimin-coated latex beads. Recombinant glutathione *S* -transferase (GST) and GST-intimin were prepared as described previously (36). Latex beads (Sekisui Chemical Co., Ltd.; average diameter, 0.993 μm) suspended in PBS at a concentration of 2×10^{10} beads/ml were mixed with an equal volume of 100 μg/ml of purified recombinant GST or GST-intimin and incubated for 80 min at 4°C. The beads were then incubated in PBS–0.1% bovine serum albumin (BSA) for 60 min at 4°C, washed with PBS three times, and suspended in 0.5 ml of PBS-BSA at a final density of 4.0×10^9 beads/ml. Monolayers of Caco/B7 cells on Transwells were preinfected with an intimin-deficient mutant of EPEC (Δ *eae*) at an MOI of 100 and incubated for 1 h at 37°C in a CO_2 incubator. After the incubation, nonadherent bacteria were removed by gentle washing with DMEM three times. The cells were treated with the intimin-coated beads at a ratio of 400 beads per cell at 37°C in a CO_2 incubator. The treated cells were fixed and stained for ZO-1 and F-actin, as described below. The number of ZO-1- or F-actin-positive beads was counted under a microscope and is represented as a percentage of the total number of beads in the field.

Antibody-mediated clustering of membrane-targeted Nck SH3 domains (Nck clustering assay). Clustering of membrane-targeted Nck SH3 domains was performed by antibody-mediated cross-linking of forms of CD16/7 fused with Nck SH3 domains as described previously (44). NIH 3T3 cells expressing the fusion proteins were incubated with a rat monoclonal antibody against human CD16 in DMEM–10% FBS for 1 h at 37°C. After being washed with prewarmed serum-free DMEM three times, the cells were reacted with Alexa 546-conjugated anti-rat immunoglobulin G (IgG) in DMEM–10% FBS for an additional hour at 37°C. The cells were fixed and stained with Alexa 488-phalloidin, T8-754, and Alexa 488-conjugated anti-mouse IgG antibody, as described below.

Immunofluorescence microscopy. The cells on the filter support or the coverglass were washed three times with DMEM and fixed with 4% paraformaldehyde in PBS for 20 min at room temperature. After permeabilization with 0.1% Triton X-100 in PBS for 10 min, the cells were incubated with PBS(+)-BSA (PBS containing 0.1%BSA, 2 mM $CaCl_2$, and 0.5 mM $MgCl_2$) for 10 min and then with the primary antibodies diluted with PBS(+)-BSA for 60 min at room temperature. After being washed with PBS, the samples were allowed to react with the secondary antibodies diluted with PBS(+)-BSA for 60 min at room temperature together with rhodamine-phalloidin (Invitrogen) to stain F-actin. When necessary, bacteria and cell nuclei were stained with 4′,6′-diamidino-2-phenylindole (DAPI; Invitrogen). The rabbit anti-intimin antibody was prepared as described previously (36). Anti-ZO-1 mouse monoclonal antibody (T8-754) was a gift from Sho-ichiro Tsukita, Kyoto University. The antiphosphotyrosine monoclonal antibody 4G10 was purchased from Upstate, Inc. Anti-O127 rabbit serum was from Denka Seiken Co., Ltd. The secondary antibodies conjugated with Alexa 350, Alexa 488, or Alexa 546 were purchased from Invitrogen.

The expression of NZO-1 was detected by immunostaining with anti-VSVG goat antibody (Abcam, Inc.) and anti-goat IgG conjugated with Alexa 488. The expression of CZO-1 and its truncated forms was detected by the fluorescence of mEGFP. The expression and aggregation of CD16/7 fusion proteins were detected with anti-human CD16 rat antibody (Serotec, Ltd.) and anti-rat IgG conjugated with Alexa 546.

The immunostained samples were mounted in Perma Fluor aqueous mounting medium (Shandon/Lipshaw, Pittsburgh, PA) and observed with an epifluorescence microscope (model BX50; Olympus). Images were collected and analyzed with Photometrics Cool SNAP HQ (Roper Scientific) and Photoshop (Adobe).

RESULTS

EPEC recruits ZO-1 to the bacterial attachment sites, dependent on the bacterial factors Tir and intimin. We examined if ZO-1 in the tight junctions of polarized Caco/B7 monolayers is aberrantly redistributed by EPEC infection. Uninfected Caco/B7 monolayers exhibited staining of ZO-1 with a well-defined honeycomb pattern in the perijunctional region (Fig. 1A). Upon infection by EPEC, the peripheral lining of ZO-1 began to disperse at 3 h postinfection and became discontinuous at 5 h or later. These changes are basically consistent with the observations made with T84 monolayers (10, 37, 43, 48). In addition to these changes, we noticed the recruitment of ZO-1 to the sites of bacterial attachment (Fig. 1B and C). To examine the bacterial factors involved in this phenomenon, we used two TTSS mutants: a Δ *escC* mutant and a Δ *espA* mutant (39). Infection of Caco/B7 monolayers by either mutant failed to induce the recruitment (Fig. 1D) (data not shown), indicating that "effectors" secreted through TTSS (24) mediate the recruitment. We then focused on an effector, Tir, and an outer membrane adhesin, intimin, because these are the inducers of the localized cytoskeletal reorganization beneath the adhered bacteria (7, 28). As a result, neither a *tir*-deficient (Δ*tir*) mutant nor the Δ*eae* mutant triggered recruitment of ZO-1 (Fig. 1D). A control *espF*-deficient strain that is partially defective in barrier-disrupting activity, but is able to induce actin polymerization (34), did induce the recruitment, as the wild-type EPEC did (data not shown). The expression of the respective gene in the Δ*tir* or Δ*eae* mutant from plasmids restored the ability to recruit ZO-1 (data not shown). These results collectively suggest the importance of the binding of Tir with intimin for the recruitment of ZO-1.

To exclude the possibility that Tir and intimin are required, but not sufficient, to induce the recruitment of ZO-1, we employed a "primed-and-challenge" method (42), in which Caco/B7 monolayers were infected by the Δ*eae* mutant (priming) and thereafter allowed to react with latex beads coated with recombinant intimin (challenge). Figure 1E shows the intimin bead-induced actin polymerization and ZO-1 recruitment, which indicates that the clustering of the Tir-intimin complex on artificial particles is sufficient for ZO-1's recruitment. It was noted that the beads stained positive for F-actin [F-actin(+)] were not necessarily colocalized with ZO-1, although all the beads stained positive for ZO-1 were colocalized with F-actin [F-actin(+)/ZO-1(+)]. Quantification revealed that 46.7% of the attached beads were F-actin(+), whereas only 8.5% were F-actin(+)/ZO-1(+), at 3 h postinfection (Fig. 1F). These ratios increased with time, reaching 78.8% for F-actin(+) and 55.5% for F-actin(+)/ZO-1(+) beads, at 7 h postinfection. A control that had adsorbed GST rarely adhered to the Δ *eae* mutant-primed monolayer and caused no localized actin polymerization (data not shown).

ZO-1 is incorporated within the pedestal, showing a distinctive distribution pattern. The results shown in Fig. 1F suggest that ZO-1 is associated with the preformed actin-rich pedestals. We next investigated the topology of ZO-1 within the pedestals. HeLa cells were used for these experiments, because 1- to 5-μm-long projections over plasma membranes develop at a high efficiency with this cell line (16). Visualization of ZO-1 in the membranous protrusions revealed that the protein is incorporated within the pedestal body (Fig. 1G). It should be noted that ZO-1 accumulated most in the distal part of the structure and was only faintly stained in the proximal part.

To confirm if the F-actin bundles are indeed necessary for the recruitment, we used a mutant, Tir(Y474F), in which tyrosine at position 474 is replaced by phenylalanine. Previous investigations revealed that binding of intimin with Tir results in the phosphorylation of Y474 (26) and that the phosphorylation is required for the recruitment and clustering of the host adaptor protein Nck beneath the attached bacterium and for the subsequent activation of the N-WASP–Arp2/3 pathway (19, 23). As a result, neither ZO-1 accumulation nor actin polymerization was observed with the Δ *tir* mutant expressing Tir(Y474F), whereas the Δ *tir* mutant expressing a wild-type

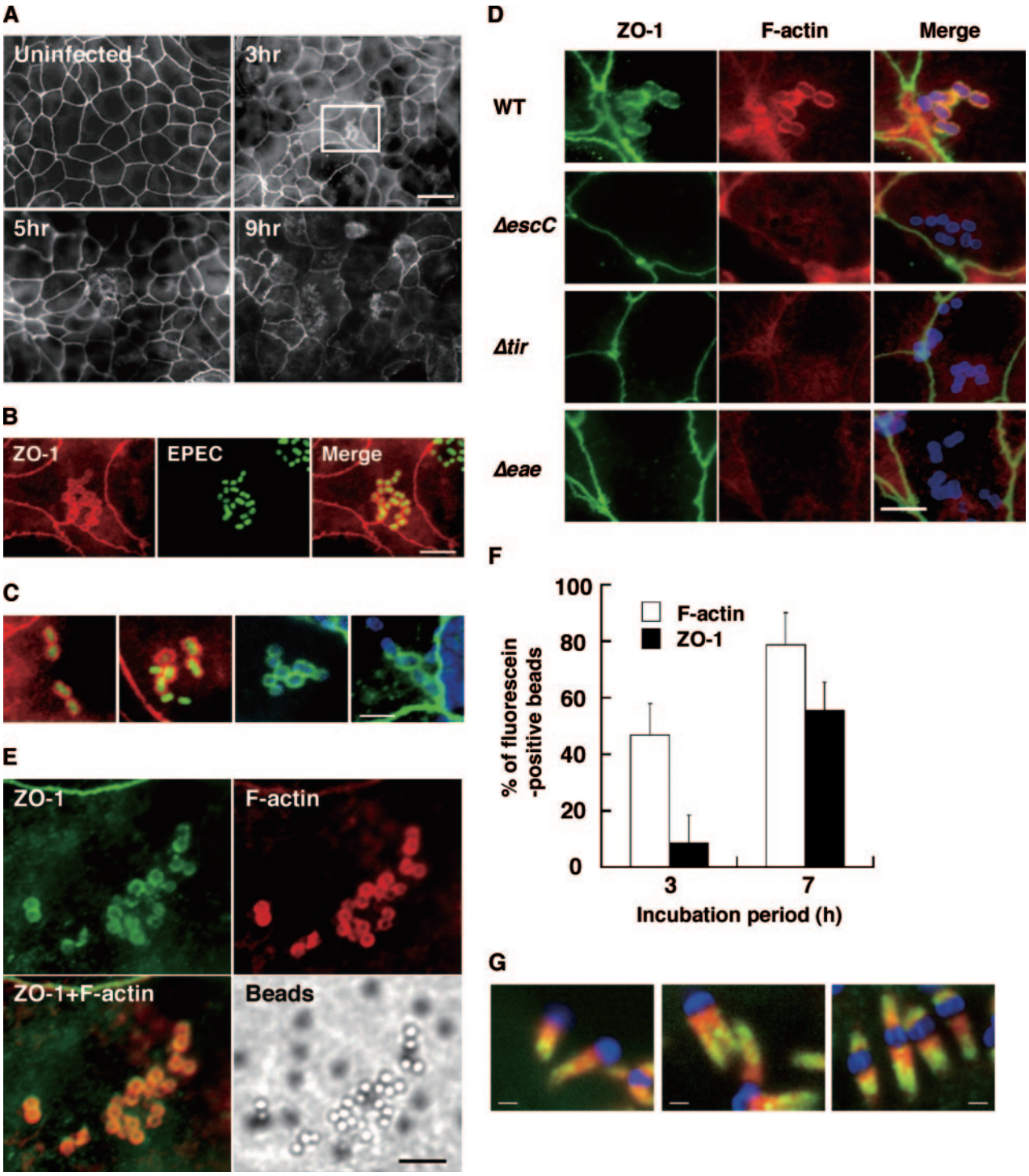

FIG. 1. EPEC recruits ZO-1 to site of the bacterial attachment and to the distal part of the pedestal body. (A) Time course of changes in the localization of ZO-1 in Caco/B7 monolayers infected by EPEC. An uninfected monolayer and monolayers infected with EPEC for 3 h, 5 h, or 9 h were fixed and stained for ZO-1 as described in Materials and Methods. It is notable that the infection caused an irregular and discontinuous ZO-1 staining at intercellular junctions. Scale bar, 20 μm. (B) A higher magnification of the region boxed in white lines in panel A (3hr). ZO-1 was stained with anti-ZO-1 antibody (left panel, red), and wild-type EPEC was stained with anti-intimin polyclonal antibody (center panel, green). A composite image is shown on the right. Scale bar, 5 μm. (C) ZO-1's recruitment to the bacterial attachment sites. Cells infected with EPEC for 3 h were fixed and subjected to immunostaining with different fluorescein reagents as follows. EPEC was stained with anti-intimin antibody (two panels on the left; green) or with DAPI (two panels on the right; blue). ZO-1 was first labeled with T8-754 and visualized with Alexa 546-conjugated secondary antibody (two panels on the left; red) or with Alexa 488-conjugated secondary antibody (two panels on the right; green). Scale bar, 3 μm. (D) TTSS, Tir, and intimin are required for the EPEC-induced recruitment of ZO-1. Caco/B7 monolayers cultured on filter supports were infected with EPEC wild-type (WT) or mutant strains for 3 h. The cells were fixed and stained for ZO-1 with anti-ZO-1 antibody (green) and for F-actin with rhodamine-phalloidin (red). The bacteria adhered on the cells were stained either with anti-intimin antibody (wild type and Δ *escC*

Tir caused both the accumulation and the formation of pedestals (see Fig. S1A and B in the supplemental material). The results demonstrate the necessity of the phosphorylation-dependent formation of pedestals for the recruitment of ZO-1.

The recruitment of ZO-1 is not involved in the EPEC-induced disruption of the epithelial barrier. Amieva and colleagues have reported that *Helicobacter pylori* causes a similar recruitment of ZO-1 to the bacterial attachment sites in Madin-Darby canine kidney (MDCK) cell monolayers and proposed that the recruitment is linked to a dysfunctional paracellular seal (1). Because EPEC has been reported to affect the integrity of the epithelial barrier (11, 32, 34, 36, 37, 43, 54), we examined if the EPEC-induced recruitment of ZO-1 is also linked with the disruption of the barrier. A polarized Caco/B7 monolayer was infected with wild-type EPEC and the mutants, and the TER across the monolayer, which is a hallmark of the integrity of the epithelial barrier, was measured. As reported previously (36), the wild-type EPEC induced a decrease of TER, whereas the Δ *tir* strain did not (see Fig. S1C in the supplemental material). The expression of a wild-type Tir in the Δ *tir* mutant restored the barrier-disrupting ability. Notably, the expression of a mutant Tir(Y474F) in Δ *tir* also restored the ability (see Fig. S1C in the supplemental material); nevertheless, the strain does not induce ZO-1's recruitment (see Fig. S1A and B in the supplemental material). The results demonstrate that the process for the recruitment is not linked with the EPEC-induced disruption of the epithelial barrier.

The PRR of ZO-1 mediates the recruitment to the pedestals. ZO-1 is a member of the membrane-associated guanylate kinase homologue family (15, 55), and possesses three PDZ domains, an SH3 domain, a noncatalytic guanylate kinase (Guk) homology domain, an acidic domain and a basic domain, and a proline-rich C terminus (15) (Fig. 2A). To understand the functional implications of ZO-1's recruitment, we dissected ZO-1's structure and tried to identify the region involved in the recruitment process. First, the ZO-1 molecule was divided into two fragments, NZO-1 and CZO-1, at an immediate C terminus of the third PDZ domain (Fig. 2A). When expressed in HeLa cells, NZO-1 showed a diffuse distribution within the cytoplasm. Even after the cells were infected by the wild-type EPEC, no accumulation of this protein within the pedestals was observed (Fig. 2B). In contrast, CZO-1 was recruited and concentrated within the pedestals induced to form by EPEC (Fig. 2C). Truncation of the SH3 or Guk domain in CZO-1 did not affect the pattern of distribution (Fig. 2D and E), indicating that these domains are dispensable for the recruitment. On the other hand, truncation of the proline-rich region (PRR; amino acids 762 to 1746) abolished the ability of CZO-1 to be recruited to the pedestals (Fig. 2F). Also, the region alone accumulated within the pedestals (Fig. 2G), suggesting that the recruitment of ZO-1 to the pedestals was mediated by the proline-rich region.

***Shigella* and *Listeria* also recruit ZO-1 to the actin tails through the proline-rich region.** Next we asked whether *S. flexneri* and *L. monocytogenes* induce a similar recruitment. When HeLa cells were infected by these bacteria, cytoplasmic actin tails extending from one pole of a bacterial cell were clearly detectable with phalloidin staining (Fig. 2I). Visualization of ZO-1 with the anti-ZO-1 monoclonal antibody T8-754 revealed the colocalization of the protein with the actin tails. Notably, the intensity of ZO-1 was greater in the distal part of the actin tail, as observed in the EPEC-induced pedestals. Figure 2J shows that the recruitment of ZO-1 to the actin tails was also mediated by the proline-rich region. The NZO-1 or control mEGFP expressed in HeLa cells did not accumulate in the tails induced to form either by *S. flexneri* or by *L. monocytogenes* (see Fig. S2 in the supplemental material), demonstrating that the region mediates the recruitment of ZO-1 to the actin tails created by *Shigella* and *Listeria*.

Nck clustering is sufficient to trigger actin polymerization and ZO-1 recruitment. A common feature among the processes of actin polymerization induced by the three bacteria is the activation of the N-WASP-related proteins and subsequent activation of the Arp2/3 complex (18). To examine if this common signal is a trigger for ZO-1's recruitment, we used an Nck clustering assay. The assay uses the three tandem SH3 domains of Nck, expressed as a chimera fused with the extracellular and transmembrane domains of the human immunoglobulin Fc receptors CD16 and CD7, respectively. Treatment of the cells expressing this chimera [Nck SH3(1+2+3)] with anti-CD16 rat antibody and anti-rat IgG antibody induces clustering of Nck SH3(1+2+3) at the cytoplasmic face of the plasma membrane, thereby triggering actin polymerization through N-WASP's activation. On the other hand, treatment of the cells expressing a control chimera, Nck SH3(3), that lacks two N-terminal SH3 domains but possesses a single SH3(3) domain, does not activate the signal (44). We caused NIH 3T3 cells to express the chimeric proteins and treated them with clustering-inducing antibodies. The treatment induced the clustering of the fusion protein and the formation of green actin tails extending from the clusters (Fig. 2K, upper panel), whereas the treatment of

and Δ *tir* mutants) or with anti-O127 antiserum (Δ *eae* mutant) and visualized with Alexa 350-conjugated anti-rabbit IgG antibody (blue). Scale bar, 5 μm. (E) Binding of intimin-coated beads to the translocated Tir on the cell surface induces actin polymerization and the recruitment of ZO-1. Caco/B7 monolayers were primed by infection with Δ*eae* mutant for 1 h. Then the monolayers were washed and challenged with latex beads coated with GST-intimin fusion protein. The monolayers were subjected to staining for ZO-1 and F-actin with anti-ZO-1 antibody (green) and rhodamine-phalloidin (red), respectively, at 7 h postchallenge. Latex beads were detected under a phase-contrast microscope. Scale bar, 5 μm. (F) Quantitative analysis of actin condensation and recruitment of ZO-1, induced at the intimin-coated beads. The open bar represents the percentage of beads showing actin condensation, and the filled bar represents the percentage of those showing ZO-1 recruitment. Ten microscopic fields were randomly selected for the quantification per sample, and a total of 60 to 200 beads were counted per field. Data represent the means (± standard deviation) from three independent experiments. (G) Localization of ZO-1 within the pedestals produced in HeLa cells infected by wild-type EPEC. It is notable that ZO-1 (green) is accumulated in the distal part of the pedestals and is excluded from the area proximate to the attached bacterium. F-actin is stained with rhodamine-phalloidin (red), and the bacteria were stained with rabbit anti-intimin serum and Alexa 350-conjigated anti-rabbit IgG antibody (blue). Bars, 1 μm.

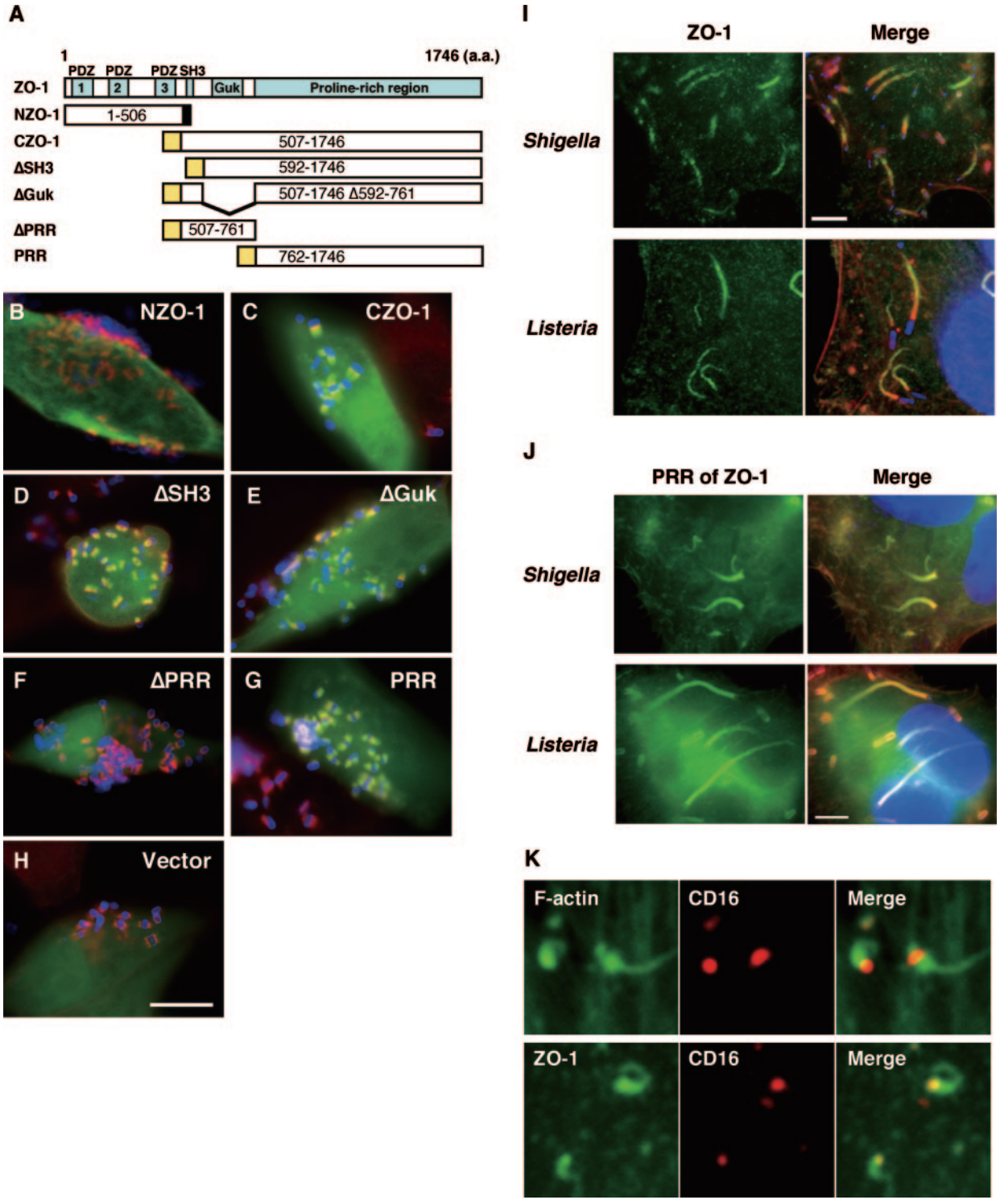

FIG. 2. Recruitment of ZO-1 to the actin-rich structures induced by three pathogens is mediated through the PRR of ZO-1 and is triggered by a WASP-related signal. (A) Schematic representation of the entire ZO-1 and the truncated forms of ZO-1 used in this study. A ZO-1 mutant with the N-terminal half (NZO-1) was tagged at the C terminus with a VSVG epitope (black box). The other mutants with the C-terminal half of ZO-1 (CZO-1, ΔSH3, ΔGuk, ΔPRR, and PRR) were fused to mEGFP at their N termini (yellow box). The numbers in each box represent the positions of amino acids corresponding to the entire mouse ZO-1 sequence. (B to H) HeLa cells expressing exogenous ZO-1 mutants were infected with wild-type EPEC for 3 h. After treatment with gentamicin (100 μg/ml) for 3 h, the cells were fixed and stained for F-actin with rhodamine-phalloidin (red) and for the bacteria with anti-intimin antibody and Alexa 350–anti-rabbit IgG (blue). The expression of the ZO-1 mutant was detected with anti-VSVG tag antibody (NZO-1, panel B) or the green fluorescence of mEGFP (C to H). For a control, the cells transfected with control vector (pcDNA3mEGFP-C) are also shown (H). Scale bar, 10 μm. (I) ZO-1 is recruited to the actin comets created by *S. flexneri* and *L. monocytogenes*. HeLa cells were infected by either *S. flexneri* or *L. monocytogenes* as described in Materials and Methods. The cells were fixed and

the cells expressing the control chimera with the antibodies did not (see Fig. S3A in the supplemental material). Next, we similarly treated the cells and stained them with anti-ZO-1 antibody, T8-754. Tail-like structures that were morphologically indistinguishable from the actin tails were observed with the cells expressing Nck SH3(1+2+3) (Fig. 2K, lower panel). In contrast, control cells expressing SH3(3) did not have "ZO-1 tails" created by the clustering-inducing antibodies (see Fig. S3B in the supplemental material). The results indicate that the clustering of Nck SH3 domains sufficiently induces localized actin polymerization and subsequent recruitment of ZO-1 and that this process requires no EPEC factors once Nck is clustered within a distinct region.

DISCUSSION

In the present study, we found that EPEC causes the recruitment of ZO-1 to the site where the bacterium attaches on the host cell and that the recruitment depends on the bacterial virulence factors Tir and intimin. We demonstrated that the binding between these proteins and the subsequent formation of F-actin bundles are prerequisites for the recruitment. Additionally, our immunocytochemical experiments revealed that ZO-1 is incorporated within EPEC-induced F-actin bundles, especially in the distal part of the structure, through the C-terminal proline-rich region of the ZO-1 molecule. A similar recruitment of ZO-1 was observed within the actin tails created by *S. flexneri* and *L. monocytogenes*. Again, ZO-1 was specifically distributed in the distal part of the actin tail through the proline-rich region.

The significance of the recruitment to the bacterial pathogenesis was examined, focusing on the EPEC-induced disruption of the epithelial barrier. It turned out that the disruption was unrelated to the recruitment. The implications for other pathological effects of the bacteria are currently under investigation, using ZO-1-deficient mutant cultured mouse epithelial cells (57). Preliminary results revealed that the incidence and the morphology of the pedestals and the motility of *Shigella* in the cells are not significantly altered in the mutant cells (our unpublished observations). We speculate that this is due to the functional redundancy between ZO-1 and ZO-2, another member of the membrane-associated guanylate kinase homologue family (15). The speculation is strongly supported by a recent report describing that in the absence of ZO-1, some physiological functions of ZO-1 are compensated for by ZO-2 in the polarized epithelial cells (56). We confirmed that ZO-2 is expressed in Caco/B7 and HeLa cells and is also recruited to the pedestals and the actin tails (our unpublished observation). The study to clarify the biological significance of the recruitment using the cells lacking the expression of both ZO-1 and ZO-2 (56) is now in progress.

To our knowledge, we have shown for the first time that ZO-1 is recruited to the pathogen-created actin-rich structures. ZO-1 generally concentrates at tight junctions or spot-like adherens junctions (21, 22, 50) or in the nucleus of dividing cells (17). It is not usually accumulated within other actin-rich structures such as stress fibers and filopodia. The reason why ZO-1 is concentrated only within particular cytoskeletal structures like junctional complexes currently remains obscure. Therefore, understanding the mechanism of ZO-1's recruitment is of great interest in terms of cell biology. One approach to understanding this mechanism would be to identify the molecule directly bound with ZO-1. In this study, we demonstrated that the proline-rich region is responsible for the recruitment. It has been reported that within the region, ZO-1 possesses an F-actin-binding site (ABS; amino acids 1157 to 1371) (13). This had raised the possibility that ABS is involved in the recruitment of ZO-1. The possibility, however, was considered unlikely, since a truncated form of CZO-1, which lacks an entire ABS, still accumulated in the EPEC-induced pedestals (our unpublished observation). We speculate that the ZO-1 in the pedestals or actin tails associates with other structural components that are specifically incorporated within the particular actin-rich structures. Our finding that ZO-1 is recruited to the distal part of the localized F-actin bundles could be a clue to identifying the ZO-1-binding proteins within the structures.

Another approach to understanding the mechanism of ZO-1's recruitment is to search for a common trigger for the formation of particular F-actin bundles that bind with ZO-1. In this study, we demonstrated that three pathogens created ZO-1-associated actin-rich structures, which commonly occur downstream of a WASP-related signaling pathway. To test the notion that the signal is tightly coupled with ZO-1's recruitment, we performed an Nck clustering assay and found that the clustering induced the recruitment of ZO-1 to the actin comets. Thus, the signal appears to be a key to the recruitment. WASP-mediated actin polymerization has been observed in a variety of biological processes, such as the formation of an actin ring at the immunological synapse (2), the growth factor-stimulated changes in cell shape and migration (14, 25), and the vesicle-propelling effect upon overexpression of phosphatidylinositol-4-phosphate 5-kinase (4). Understanding whether ZO-1 is also recruited during these processes and whether ZO-1 is required for these processes is important to differentiate the ZO-1-bound actin-rich structures from the structures without ZO-1.

In conclusion, we have shown that the pathogenic bacteria used in this study recruit ZO-1 to the unique actin-rich structures termed actin tails and pedestals. Although the role of the recruitment in the bacterial pathogenesis is currently unknown,

stained for endogenous ZO-1 (green) and for F-actin (red). The infected bacteria were visualized with DAPI (blue). Scale bars, 5 μm. (J) The PRR of ZO-1 mediates the recruitment of ZO-1 to the actin comets generated by *S. flexneri* and *L. monocytogenes*. HeLa cells expressing mEGFP-PRR were infected with *S. flexneri* (upper panel) or *L. monocytogenes* (lower panel) as described in Materials and Methods. Cells were fixed and stained for F-actin with rhodamine-phalloidin (red) and for the infected bacteria with DAPI (blue). Scale bar, 5 μm. (K) Clustering of the membrane-targeted Nck SH3 domains induces the recruitment of ZO-1 and formation of actin tails. NIH 3T3 cells expressing either Nck SH3(3) or Nck SH3(1+2+3) were treated with anti-CD16 and Alexa 546-conjugated anti-rat IgG antibodies. After fixation, the clustered fusion proteins were visualized (red). F-actin and ZO-1 were visualized with Alexa 488-phalloidin (upper panel, green) and anti-ZO-1 antibody (lower panel, green).

analysis of this phenomenon may unveil a novel role of ZO-1 in the pathological effect of the bacteria. In addition, the recruitment of ZO-1 to the particular F-actin bundles is of great interest, because the mechanism regulating the cellular localization of ZO-1 is largely unknown. Further investigation, using the experimental systems described in this study, will lead to an understanding of the roles of ZO-1 in actin dynamics and of the mechanism regulating the localization of ZO-1 during the reorganization of the cytoskeletal network.

ACKNOWLEDGMENTS

This work was supported by Grants-in-Aid for Scientific Research on Priority Areas (no. 12144208 and 16017255) and for Scientific Research (B) (no. 15390142) from the Ministry of Education, Culture, Sport, Science, and Technology of Japan and by the Combined Program on Microbiology and Immunology, the 21st Century COE Program.

We thank Sho-ichiro Tsukita, Teruhito Yasui, and Bruce J. Mayer for providing DNA constructs and a monoclonal antibody and Kazuko Seto, Teizo Tsukamoto, Junko Matsuyama, and Myonsan Yoh for providing the clinical isolates of *S. flexneri* and *L. monocytogenes*. We are also grateful to Sami Fujihara and Kuniko Ishiguro for their technical and secretarial assistance.

REFERENCES

1. **Amieva, M. R., R. Vogelmann, A. Covacci, L. S. Tompkins, W. J. Nelson, and S. Falkow.** 2003. Disruption of the epithelial apical-junctional complex by *Helicobacter pylori* CagA. Science **300:** 1430–1434.
2. **Barda-Saad, M., A. Braiman, R. Titerence, S. C. Bunnell, V. A. Barr, and L. E. Samelson.** 2005. Dynamic molecular interactions linking the T cell antigen receptor to the actin cytoskeleton. Nat. Immunol. **6:** 80–89.
3. **Batchelor, M., J. Guignot, A. Patel, N. Cummings, J. Cleary, S. Knutton, D. W. Holden, I. Connerton, and G. Frankel.** 2004. Involvement of the intermediate filament protein cytokeratin-18 in actin pedestal formation during EPEC infection. EMBO Rep. **5:** 104–110.
4. **Benesch, S., S. Lommel, A. Steffen, T. E. Stradal, N. Scaplehorn, M. Way, J. Wehland, and K. Rottner.** 2002. Phosphatidylinositol 4,5-biphosphate (PIP2)-induced vesicle movement depends on N-WASP and involves Nck, WIP, and Grb2. J. Biol. Chem. **277:** 37771–37776.
5. **Bernardini, M. L., J. Mounier, H. D'Hauteville, M. Coquis-Rondon, and P. J. Sansonetti.** 1989. Identification of *icsA*, a plasmid locus of *Shigella flexneri* that governs bacterial intra- and intercellular spread through interaction with F-actin. Proc. Natl. Acad. Sci. USA **86:** 3867–3871.
6. **Boujemaa-Paterski, R., E. Gouin, G. Hansen, S. Samarin, C. Le Clainche, D. Didry, P. Dehoux, P. Cossart, C. Kocks, M. F. Carlier, and D. Pantaloni.** 2001. *Listeria* protein ActA mimics WASp family proteins: it activates filament barbed end branching by Arp2/3 complex. Biochemistry **40:** 11390–11404.
7. **Campellone, K. G., S. Rankin, T. Pawson, M. W. Kirschner, D. J. Tipper, and J. M. Leong.** 2004. Clustering of Nck by a 12-residue Tir phosphopeptide is sufficient to trigger localized actin assembly. J. Cell Biol. **164:** 407–416.
8. **Cantarelli, V. V., T. Kodama, N. Nijstad, S. K. Abolghait, T. Iida, and T. Honda.** 2006. Cortactin is essential for F-actin assembly in enteropathogenic *Escherichia coli* (EPEC)- and enterohaemorrhagic *E. coli* (EHEC)-induced pedestals and the alpha-helical region is involved in the localization of cortactin to bacterial attachment sites. Cell Microbiol. **8:** 769–780.
9. **Cantarelli, V. V., A. Takahashi, I. Yanagihara, Y. Akeda, K. Imura, T. Kodama, G. Kono, Y. Sato, and T. Honda.** 2001. Talin, a host cell protein, interacts directly with the translocated intimin receptor, Tir, of enteropathogenic *Escherichia coli*, and is essential for pedestal formation. Cell Microbiol. **3:** 745–751.
10. **Czerucka, D., S. Dahan, B. Mograbi, B. Rossi, and P. Rampal.** 2000. *Saccharomyces boulardii* preserves the barrier function and modulates the signal transduction pathway induced in enteropathogenic *Escherichia coli* -infected T84 cells. Infect. Immun. **68:** 5998–6004.
11. **Dean, P., and B. Kenny.** 2004. Intestinal barrier dysfunction by enteropathogenic *Escherichia coli* is mediated by two effector molecules and a bacterial surface protein. Mol. Microbiol. **54:** 665–675.
12. **Dold, F. G., J. M. Sanger, and J. W. Sanger.** 1994. Intact alpha-actinin molecules are needed for both the assembly of actin into the tails and the locomotion of *Listeria monocytogenes* inside infected cells. Cell Motil. Cytoskelet. **28:** 97–107.
13. **Fanning, A. S., T. Y. Ma, and J. M. Anderson.** 2002. Isolation and functional characterization of the actin binding region in the tight junction protein ZO-1. FASEB J. **16:** 1835–1837.
14. **Gong, C., K. V. Stoletov, and B. I. Terman.** 2004. VEGF treatment induces signaling pathways that regulate both actin polymerization and depolymerization. Angiogenesis **7:** 313–321.
15. **González-Mariscal, L., A. Betanzos, and A. Ávila-Flores.** 2000. MAGUK proteins: structure and role in the tight junction. Semin. Cell Dev. Biol. **11:** 315–324.
16. **Goosney, D. L., R. DeVinney, and B. B. Finlay.** 2001. Recruitment of cytoskeletal and signaling proteins to enteropathogenic and enterohemorrhagic *Escherichia coli* pedestals. Infect. Immun. **69:** 3315–3322.
17. **Gottardi, C. J., M. Arpin, A. S. Fanning, and D. Louvard.** 1996. The junction-associated protein, zonula occludens-1, localizes to the nucleus before the maturation and during the remodeling of cell-cell contacts. Proc. Natl. Acad. Sci. USA **93:** 10779–10784.
18. **Gouin, E., M. D. Welch, and P. Cossart.** 2005. Actin-based motility of intracellular pathogens. Curr. Opin. Microbiol. **8:** 35–45.
19. **Gruenheid, S., R. DeVinney, F. Bladt, D. Goosnet, S. Gelkop, G. D. Gish, T. Pawson, and B. B. Finlay.** 2001. Enteropathogenic *E. coli* Tir binds Nck to initiate actin pedestal formation in host cells. Nat. Cell Biol. **3:** 856–859.
20. **Gruenheid, S., and B. B. Finlay.** 2003. Microbial pathogenesis and cytoskeletal function. Nature **422:** 775–781.
21. **Itoh, M., M. Furuse, K. Morita, K. Kubota, M. Saitou, and S. Tsukita.** 1999. Direct binding of three tight junction-associated MAGUKs, ZO-1, ZO-2, and ZO-3, with the COOH termini of claudins. J. Cell Biol. **147:** 1351–1363.
22. **Itoh, M., A. Nagafuchi, S. Yonemura, T. Kitani-Yasuda, S. Tsukita, and S. Tsukita.** 1993. The 220-kD protein colocalizing with cadherins in nonepithelial cells is identical to ZO-1, a tight junction-associated protein in epithelial cells: cDNA cloning and immunoelectron microscopy. J. Cell Biol. **121:** 491–502.
23. **Kalman, K., O. D. Weiner, D. L. Goosney, J. W. Sedat, B. B. Finlay, A. Abo, and J. M. Bishop.** 1999. Enteropathogenic *E. coli* acts through WASP and Arp2/3 complex to form actin pedestals. Nat. Cell Biol. **1:** 389–391.
24. **Kaper, J. B., J. P. Nataro, and H. L. T. Mobley.** 2004. Pathogenic *Escherichia coli*. Nat. Rev. Microbiol. **2:** 123–140.
25. **Kempiak, S. J., H. Yamaguchi, C. Sarmiento, M. Sidani, M. Ghosh, R. J. Eddy, V. Desmarais, M. Way, J. Condeelis, and J. E. Segall.** 2005. A neural Wiskott-Aldrich Syndrome protein-mediated pathway for localized activation of actin polymerization that is regulated by cortactin. J. Biol. Chem. **280:** 5836–5842.
26. **Kenny, B.** 1999. Phosphorylation of tyrosine 474 of the enteropathogenic *Escherichia coli* (EPEC) Tir receptor molecule is essential for actin nucleating activity and is preceded by additional host modifications. Mol. Microbiol. **31:** 1229–1241.
27. **Levine, M. M., E. J. Bergquist, D. R. Nalin, D. H. Waterman, R. B. Hornick, C. R. Young, and S. Sotman.** 1978. *Escherichia coli* strains that cause diarrhoea but do not produce heat-labile or heat-stable enterotoxins and are non-invasive. Lancet **i:** 1119–1122.
28. **Liu, H., L. Magoun, S. Luperchio, D. B. Schauer, and J. M. Leong.** 1999. The Tir-binding region of enteropathogenic *Escherichia coli* intimin is sufficient to trigger actin condensation after bacterial-induced host cell signalling. Mol. Microbiol. **34:** 67–81.
29. **Loisel, T. P., R. Boujemaa, D. Pantaloni, and M. F. Carlier.** 1999. Reconstitution of actin-based motility of *Listeria* and *Shigella* using pure proteins. Nature **401:** 613–616.
30. **Lommel, S., S. Benesch, K. Rottner, T. Franz, J. Wehland, and R. Kühn.** 2001. Actin pedestal formation by enteropathogenic *Escherichia coli* and intracellular motility of *Shigella flexneri* are abolished in N-WASP-defective cells. EMBO Rep. **2:** 850–857.
31. **Luo, Y., E. A. Frey, R. A. Pfuetzner, A. L. Creagh, D. G. Knoechel, C. A. Haynes, B. B. Finlay, and N. C. J. Strynadka.** 2000. Crystal structure of enteropathogenic *Escherichia coli* intimin-receptor complex. Nature **405:** 1073–1077.
32. **Matsuzawa, T., A. Kuwae, and A. Abe.** 2005. Enteropathogenic *Escherichia coli* type III effectors EspG and EspG2 alter epithelial paracellular permeability. Infect. Immun. **73:** 6283–6289.
33. **Matsuzawa, T., A. Kuwae, S. Yoshida, C. Sasakawa, and A. Abe.** 2004. Enteropathogenic *Escherichia coli* activates the RhoA signaling pathway via the stimulation of GEF-H1. EMBO J. **23:** 3570–3582.
34. **McNamara, B. P., A. Koutsouris, C. B. O'Connell, J.-P. Nougayréde, M. S. Donnenberg, and G. Hecht.** 2001. Translocated EspF protein from enteropathogenic *Escherichia coli* disrupts host intestinal barrier function. J. Clin. Investig. **107:** 621–629.
35. **Mimuro, H., T. Suzuki, S. Suetsugu, H. Miki, T. Takenawa, and C. Sasakawa.** 2000. Profilin is required for sustaining efficient intra- and intercellular spreading of *Shigella flexneri*. J. Biol. Chem. **275:** 28893–28901.
36. **Miyake, M., M. Hanajima, T. Matsuzawa, C. Kobayashi, M. Minami, A. Abe, and Y. Horiguchi.** 2005. Binding of intimin with Tir on the bacterial surface is prerequisite for the barrier disruption induced by enteropathogenic *Escherichia coli*. Biochem. Biophys. Res. Commun. **337:** 922–927.
37. **Muza-Moons, M. M., E. E. Schneeberger, and G. Hecht.** 2004. Enteropathogenic *Escherichia coli* infection leads to appearance of aberrant tight junctions strands in the lateral membrane of intestinal epithelial cells. Cell. Microbiol. **6:** 783–793.

38. **Nataro, J. P., and J. B. Kaper.** 1998. Diarrheagenic *Escherichia coli*. Clin. Microbiol. Rev. **11:** 142–201.
39. **Ogino, T., R. Ohno, K. Sekiya, A. Kuwae, T. Matsuzawa, T. Nonaka, H. Fukuda, S. Imajoh-Ohmi, and A. Abe.** 2006. Assembly of the type III secretion apparatus of enteropathogenic *Escherichia coli*. J. Bacteriol. **188:** 2801–2811.
40. **Pamer, E. G.** 2004. Immune responses to *Listeria monocytogenes*. Nat. Rev. Immunol. **4:** 812–823.
41. **Parsot, C.** 2005. *Shigella* spp. and enteroinvasive *Escherichia coli* pathogenicity factors. FEMS Microbiol. Lett. **252:** 11–18.
42. **Phillips, N., R. D. Hayward, and V. Koronakis.** 2004. Phosphorylation of the enteropathogenic *E. coli* receptor by the Src-family kinase c-Fyn triggers actin pedestal formation. Nat. Cell Biol. **6:** 618–625.
43. **Philpott, D. J., D. M. Mckay, P. M. Sherman, and M. H. Perdue.** 1996. Infection of T84 cells with enteropathogenic *Escherichia coli* alters barrier and transport functions. Am. J. Physiol. Gastrointest. Liver Physiol. **33:** G634–G645.
44. **Rivera, G. M., C. A. Briceño, F. Takeshima, S. B. Snapper, and B. J. Mayer.** 2004. Inducible clustering of membrane-targeted SH3 domains of the adaptor protein Nck triggers localized actin polymerization. Curr. Biol. **14:** 11–22.
45. **Rosenblatt, J., B. J. Agnew, H. Abe, J. R. Bamburg, and T. J. Mitchison.** 1997. *Xenopus* actin depolymerizing factor/cofilin (XAC) is responsible for the turnover of actin filaments in *Listeria monocytogenes* tails. J. Cell Biol. **136:** 1323–1332.
46. **Sekiya, K., M. Ohishi, T. Ogino, K. Tamano, C. Sasakawa, and A. Abe.** 2001. Supermolecular structure of the enteropathogenic *Escherichia coli* type III secretion system and its direct interaction with the EspA-sheath-like structure. Proc. Natl. Acad. Sci. USA **98:** 11638–11643.
47. **Shaner, N. C., J. W. Sanger, and J. M. Sanger.** 2005. Actin and alpha-actinin dynamics in the adhesion and motility of EPEC and EHEC on host cells. Cell Motil. Cytoskelet. **60:** 104–120.
48. **Simonovic, I., M. Arpin, A. Koutsouris, H. J. Falk-Krzesinski, and G. Hecht.** 2001. Enteropathogenic *Escherichia coli* activates ezrin, which participates in disruption of tight junction barrier function. Infect. Immun. **69:** 5679–5688.
49. **Stevens, J. M., E. E. Galyov, and M. P. Stevens.** 2006. Actin-dependent movement of bacterial pathogens. Nat. Rev. Microbiol. **4:** 91–101.
50. **Stevenson, B. R., J. D. Siliciano, M. S. Mooseker, and D. A. Goodenough.** 1986. Identification of ZO-1: a high molecular weight polypeptide associated with the tight junction (zonula occludens) in a variety of epithelia. J. Cell Biol. **103:** 755–766.
51. **Suzuki, T., H. Miki, T. Takenawa, and C. Sasakawa.** 1998. Neural Wiskott-Aldrich syndrome protein is implicated in the actin-based motility of *Shigella flexneri*. EMBO J. **17:** 2767–2776.
52. **Theriot, J. A., J. Rosenblatt, D. A. Portnoy, P. J. Goldschmidt-Clermont, and T. J. Mitchison.** 1994. Involvement of profilin in the actin-based motility of *L. monocytogenes* in cells and in cell-free extracts. Cell **76:** 505–517.
53. **Tilney, L. G., and D. A. Portnoy.** 1989. Actin filaments and the growth, movement, and spread of the intracellular bacterial parasite, Listeria monocytogenes. J. Cell Biol. **109:** 1597–1608.
54. **Tomson, F. L., V. K. Viswanathan, K. J. Kanack, R. P. Kanteti, K. V. Straub, M. Menet, J. B. Kaper, and G. Hecht.** 2005. Enteropathogenic *Escherichia coli* EspG disrupts microtubules and in conjunction with Orf3 enhances perturbation of the tight junction barrier. Mol. Microbiol. **56:** 447–464.
55. **Tsukita, S., M. Furuse, and M. Itoh.** 2001. Multifunctional strands in tight junctions. Nat. Rev. Mol. Cell Biol. **2:** 285–293.
56. **Umeda, K., J. Ikenouchi, S. Katahira-Tayama, K. Furuse, H. Sasaki, M. Nakayama, T. Matsui, S. Tsukita, M. Furuse, and S. Tsukita.** 2006. ZO-1 and ZO-2 independently determine where claudins are polymerized in tight-junction strand formation. Cell **126:** 741–754.
57. **Umeda, K., T. Matsui, M. Nakayama, K. Furuse, H. Sasaki, M. Furuse, and S. Tsukita.** 2004. Establishment and characterization of cultured epithelial cells lacking expression of ZO-1. J. Biol. Chem. **279:** 44785–44794.
58. **Welch, M. D., J. Rosenblatt, J. Skoble, D. A. Portnoy, and T. J. Mitchison.** 1998. Interaction of human Arp2/3 complex and the *Listeria monocytogenes* ActA protein in actin filament nucleation. Science **281:** 105–108.

Editor: A. Camilli